EFFECTS OF THE BOUNDARY CONDITIONS ON THE PROPAGATION OF PRESSURE WAVES GOVERNED BY A ONE-DIMENSIONAL LIGHTHILL-WESTERVELT EQUATION

PACS No. 43.25.-x

J. I. Ramos

Escuela de Ingenierías, Universidad de Málaga, Dr. Ortiz Ramos, s/n, 29071 Málaga, Spain, Tel. 951952387, Fax 951952452, e-mail: jirs@lcc.uma.es

ABSTRACT

Numerical studies of the effects of different impedance boundary conditions on the propagation of one-dimensional pressure waves governed by a modified Lighthill-Westervelt (LW) equation that includes a damping term whose coefficient is a function of the pressure, are reported. The boundary conditions include those corresponding to soft and hard walls, and transmission and radiation ones. For the case of Dirichlet's and transmission conditions, a steep front is formed at and bounces from the downstream boundary. It is also shown that, for the four boundary conditions considered in this study, the pressure field becomes periodic but it exhibits an initial transient whose duration depends on the magnitude of the pressure nonlinearity, the damping term, and the amplitude and frequency of the sound source.

Keywords: radiation conditions; Lighthill-Westervelt equation; wave-boundary interactions.

1   Introduction

The Lighthill-Westervelt (LW) equation [1,2] may be used to describe the nonlinear propagation of sound waves. Such an equation may be derived from the expansions of the conservation of mass, linear momentum and energy and the equation of state, and, to second-order of approximation, may be written as [3]

$$c_0^2 \, \nabla^2 p - p_{tt} + \delta \, c_0^{-1} \, p_{ttt} + \rho_0 \, c_0^{-2} \, \beta \, (p^2)_{tt} \, = 0, \qquad (1)$$

where ∇^2 is the Laplacian operator, p is the (dimensional) acoustic pressure, the third term in the left-hand side is a dissipative or lossy one due to the thermal heat conduction and the viscosity of the fluid, δ is the diffusivity of sound which is related to the sound absorption coefficient α and the frequency ω as $\delta = 2 \, \alpha \, c_0^3 \, / \, \omega^2$, t is time, ρ_0 is the (equilibrium) density of the medium, c_0 is the (equilibrium) speed of sound, β is the parameter of nonlinearity which is equal to $(\gamma + 1)/2$ and $(1 + B/(2A))$ for gases and liquids, respectively, γ is the specific heat ratio, subscripts denote differentiation, and B/A is the nonlinearity parameter [4]. The first two terms in Eq. (1) are linear and correspond to wave propagation and diffraction, the second one represents thermo-viscous losses and the last one corresponds to nonlinearities. Equation (1) with $\delta \neq 0$ is usually referred to as the lossy LW equation, whereas $\delta = 0$ corresponds to a lossless medium.

Equation (1) contains a third-order time derivative and requires that three initial conditions be specified. In addition, in the absence of nonlinearities, its dispersion relation is cubic and, therefore, has three roots, and the frequency ω is a complex number [5].

Recently, the lossy LW Eq. (1) has been used in nonlinear acoustics to improve the quality of echographic images and the deposition of heat in acoustic ablation therapy [6] due to the higher-order harmonic waves that are generated in nonlinear media, the nonlinear distortion of the acoustic field in human tissue [7], the nonlinear propagation of ultrasound beams from concave focusing sources [8,9], the distortion and harmonic generation in the near-field of finite sound sources [10], etc.

Equation (1) has been studied numerically by means of iterative techniques based on the Green's function for the linear operator of that equation, including volumetric source terms due to mass injection and forces [6,7], variable density and compressibility, operator-splittting techniques based on Padé approximations, finite differences in the time domain for a modified LW equation that accounts for attenuation and dispersion effects through the introduction of a causal convolution propagation operator [11], etc. In some of the finite difference studies of Eq. (1), it was found that a fourth-order accurate discretization of the second-order spatial derivatives was unstable and, in order to remove such an instability, a modified equation approach had to be used [11].

The lossless LW Eq. (1) has been employed to study shock wave formation in one-dimensional flows [5,12] by means of finite difference methods and has been generalized to account for losses in a phenomelogical manner [5] as

$$p_{xx} - \mu\,(p,p_t)\,p_t - (1 - 2\,\beta\,\varepsilon\,p)\,p_{tt} = -2\,\beta\,\varepsilon\,(p_t)^2, \tag{2}$$

where the term $\mu\,(p,p_t)\,p_t$ in the left-hand side of Eq. (2) with $\mu \geq 0$ accounts for losses, and $\varepsilon = V/c_0$ is the Mach number which is assumed to be small. Equation (2) is non-dimensional where (the dimensional) x, t and the velocity have been nondimensionalized with respect to L, L/c_0, and V, the acoustic density with respect to $\varepsilon\rho_0$, and V and L are characteristic values of the fluid velocity and length scale, respectively.

The losses term in Eq. (2) introduces viscous damping in a phenomenological manner, but does not introduce a third-order time derivative. The dispersion relation when such a dissipation term is employed, is a quadratic expression for the frequency as a function of the wavenumber, rather than the cubic one that would result from Eq. (1).

Equation (2) reduces to the linear wave equation for either $\varepsilon = 0$ or $\beta = 0$, i.e., for zero Mach numbers or zero nonlinearities. In such case, it is well-known that Eq. (2) has two characteristic lines along which propagation occurs, i.e., the left- and right-running waves. For nonlinear flows and non-zero Mach numbers, Eq. (2) is hyperbolic provided that $(1 - 2\,\beta\,\varepsilon\,p) > 0$, and becomes an elliptic one for $(1 - 2\,\beta\,\varepsilon\,p) \leq 0$; therefore, hyperbolic behavior occurs for nondimensional acoustic densities smaller than $1/(2\,\beta\,\varepsilon)$. Since only the product $\beta\,\varepsilon$ appears in Eq. (2), it may be stated that the nonlinearity depends on this product and, therefore, the sound propagation is a function of this product.

In one dimension, $x \in [0,1]$, and we have used the following initial conditions

$$p(0,x) = 0, \qquad p_t(0,x) = 0, \tag{3}$$

while the boundary condition at the upstream boundary is

$$p(t,0) = (-1)^{n+1} \sin(\omega\,t), \tag{4}$$

where n is a natural number or zero, while at the downstream boundary we have imposed

$$a\,p(t,1) + b\,p_x(t,1) = 0, \tag{5}$$

which correspond to Dirichlet's, Neumann's and Robin's boundary conditions for $a \neq 0$ and $b = 0$, $a = 0$ and $b \neq 0$, $a \neq 0$ and $b \neq 0$, respectively, or soft- and hard-wall and impedance/transmission boundary conditions, respectively, where a and b could be functions of

time, but have been assumed constant in this study. We have also considered the following Sommerfeld's radiation boundary condition

$$p_t(t,1) + c\,(t,1)\,p_x(t,1) = 0, \tag{6}$$

where c is a local speed to be discussed later. Unless otherwise stated, we have assumed that $\mu = \alpha\,|p|^\gamma$, where α and γ are constants, and a (nondimensional) frequency $\omega = \pi$.

2   Numerical methods and boundary conditions

Equation (2) can be written as the following system of two nonlinear, first-order differential equations

$$p_t \equiv P, \; P_t = \; [p_{xx} - \mu\,(p,P)\,P + 2\;\beta\;\varepsilon\,(P)^2]/(1 - 2\;\beta\;\varepsilon\,p), \tag{7}$$

where we have assumed that $1 - 2\,\beta\,\varepsilon\,p \neq 0$; if this condition is not met, $p = 1/(2\,\beta\,\varepsilon)$, and p_t is governed by the quadratic equation that results from Eq. (2) after imposing the condition $1 - 2\,\beta\,\varepsilon\,p = 0$. The second-order spatial derivative in Eq. (7) has been discretized by means of a three-point, fourth-order accurate, compact operator method as follows [13]

$$(G_{i-1} + \; 10\;G_i + \; G_{i+1}\,)/12 \; = \; (p_{i-1} - \; 2\;p_i + \; p_{i+1})\Delta x^2 + O(\Delta x^4), \tag{8}$$

where $G = p_{xx}$, Δx is the spatial step size, and the subscript i denotes $x_i = i\,\Delta x$. Upon applying Eq. (7) at the grid point i and using Eq. (8) in the resulting equation, a system of ordinary differential equations for the nodal values p_i and P_i is obtained and, therefore, the original partial differential Eq. (2) is transformed into a system of nonlinear ordinary differential equations by what is referred to as a method of lines. The resulting system of ordinary differential equations was solved by means of the well-known fourth-order accurate, explicit Runge-Kutta method, so that the accuracy of the resulting numerical procedure is $O(\Delta t^4,\, \Delta x^4)$ provided that the Neumann's, Robin's and Sommerfeld's boundary conditions are discretized with the same order of accuracy.

In order to achieve fourth-order accuracy when implementing Neumann's or Robin's at the downstream boundary, the pressure at nodes adjacent to that boundary was expanded in Taylor's series expansion about the pressure at that boundary, and the second-, third- and fourth-order spatial derivatives which appear in those expansions were eliminated to obtain a fourth-order accurate discretization of the first-order spatial derivative at the downstream boundary which involves the pressure there as well as the pressures at points adjacent to the downstream boundary.

In the implementation of the radiation boundary conditions given by Eq. (6), several issues arise. First, one has to decide on the local speed of sound to be used in that equation. In the first approximation followed here, the local speed of sound that appears in Eq. (6) was assumed to be unity in accord with the linear (nondimensional) wave equation; such an approach corresponds to approximating the term $(1 - 2\,\beta\,\varepsilon\,p)\,p_{tt}$ by p_{tt} in Eq. (6) and is expected to be valid provided that $|2\,\beta\,\varepsilon\,p| \ll 1$. A second approximation was based on the true local speed of sound provided by Eq. (6), i.e., $c^2\,(t,1) = 1/(1 - 2\,\beta\,\varepsilon\,p)$. The second issue that arises is the discretization of both the temporal and spatial derivatives that appear in Eq. (6) and the overall accuracy of the resulting finite difference discretization. A first-order discretization in space and time of Eq. (6), i.e.,

$$(p_N^{n+1} - \; p_N^n)/\Delta t + \; c_N\,(p_N^n - \; p_{N-1}^n)/\Delta x \; \equiv \; \partial_t p_N^n + \; c_N\,\partial_x p_N^n \; = 0, \tag{9}$$

where N denotes the grid point corresponding to the downstream boundary, i.e., $(N-1)\Delta x = 1$, the superscript n corresponds to $t^n = n\,\Delta t$, Δt denotes the time step, and and we have used equally-spaced grids in space and time, while providing an explicit expression for the pressure at the downstream boundary. Equation (9) was found to be accurate provided that the pressure

wave propagating from the upstream to the downstream boundary was sufficiently far away from the later, but introduced too much damping when the pressure wave was close to, interacted with and was reflected from the dowsntream boundary. The amount of damping and dispersion was found to decrease when an explicit, second-order accurate, finite difference discretization was used [14]; however, in this case, the overall accuracy of the method drops from $O(\Delta t^4, \Delta x^4)$ to $O(\Delta t^2, \Delta x^2)$.

In order to achieve fourth-order accuracy in both space and time when implementing the radiation boundary condition given by Eq. (6), we have employed the high-order non-reflecting boundary conditions (NRBC) operator developed by Higdon [15], i.e.,

$$\prod_{j=1}^{J}(\partial_t p_N^n + c_j \partial_x p_N^n) = 0, \tag{10}$$

where the differential operators that appear in Eq. (10) were discretized as indicated in Eq. (9). Equation (10) provides an explicit expression for p_N^{n+1}, and can be implemented to any order J by means of the following simple algorithm

$$\prod_{j=1}^{J}(a_j + d_j O_t^- + e_j O_x^-)p_N^n = 0, \tag{10}$$

where

$$a_j = 1 + c_j \frac{\Delta t}{\Delta x}, \ d_j = -1, \ e_j = -c_j \frac{\Delta t}{\Delta x}, \ O_t^- u_i^{n+1} = u_i^n, \ O_x^- u_i^n = u_{i-1}^n. \tag{12}$$

It must be pointed out that, since the problem considered in this study is one-dimensional, i.e., only plane waves are studied, c_j was taken as c_N, where, as stated above, it may be taken to be equal to one or the true local speed of sound corresponding to the right-running characteristic of Eq. (6); in multi-dimensional problems, however, the local speed c_j must be chosen so as to minimize the reflection from the downstream boundary but, if it is chosen as the wave speed of Eq. (6), the first-order condition provided by Higdon [14] is identical to Sommerfeld's radiation boundary condition, i.e., Eq. (6).

Although long-time instabilities might occur when high-order NRBC are employed because of the use of high-order derivatives (cf. Eq. (14) with $J \geq 2$), if the governing equation in the interior of the domain and the NRBC both admit solutions at zero wavenumber and frequency and if the data of the problem also include such zero modes, then a slowly growing smooth instability is possible. However, as observed by Givoli and Neta in a two-dimensional problem [16,17], whether this instability shows up in practice depends on both the order of the derivatives on the NRBC and the number of spatial dimensions; these instabilities do not arise in the presence of dispersion or if the problem data are confined to non-trivial modes.

It should also be pointed out that sometimes the implementation of Higdon's boundary conditions is referred to as the complementary operators method [18] when two solutions that employ absorbing boundary conditions (ABC) exhibit a complementary behavior, i.e., the reflection coefficients associated with the two ABC are exactly opposite to each other.

In addition to the fourth-order accurate method presented here, the time-linearization technique presented in [5] which is second-order accurate in time and fourth-order accurate in space was used with first- and second-order accurate implementations of the radiation boundary conditions and second-order spatial approximations for the downstream Neumann's and Robin's boundary conditions in order to assess the effects of time linearization and the order of accuracy in both space and time on the numerical results. The results of these numerical simulations indicate that the time-linearization method is more stable than the fourth-order accurate Runge-Kutta method presented here for the same order of spatial discretization. This is attributed to the fact that the time linearization method treats the nonlinear term on the right-hand side of Eq. (2) in an implicit, albeit linearized manner, but provides an explicit expression for the acoustic pressure, if the spatial derivatives are treated explicitly: in addition, since the coefficient of the damping term is treated explicitly, it was found that this term has a stabilizing effect on the numerical calculations.

3   Presentation of results

Figure 1 illustrates the acoustic pressure field as a function of space and time for a downstream acoustic pressure equal to zero, i.e., Dirichlet's boundary conditions, and clearly exhibits the sinusoidal pressure at the upstream boundary, an initial transient which is visible at early times near the downstream boundary. Figure 1 also shows the development of a steep pressure gradient at the downstream boundary; in fact, for $\mu = 0$, a shock wave is formed there. In the presence of damping, the results shown in Figure 1 as well as others not presented here, indicate that the pressure gradient at the downstream boundary evolves until reaching a maximum value and then decreases as the upstream boundary pressure decreases. It must be noted that the upstream boundary pressure employed in this study is positive for $t \in (m, m+1)$ with m equal to zero or even, and negative for m odd. This means that for m zero or even, there is a compression wave that propagates from the upstream to the dowstream boundary; for m odd, the pressure at the upstream boundary is negative, and an expansion or rarefaction wave is formed as shown in the left side of Figure 1.
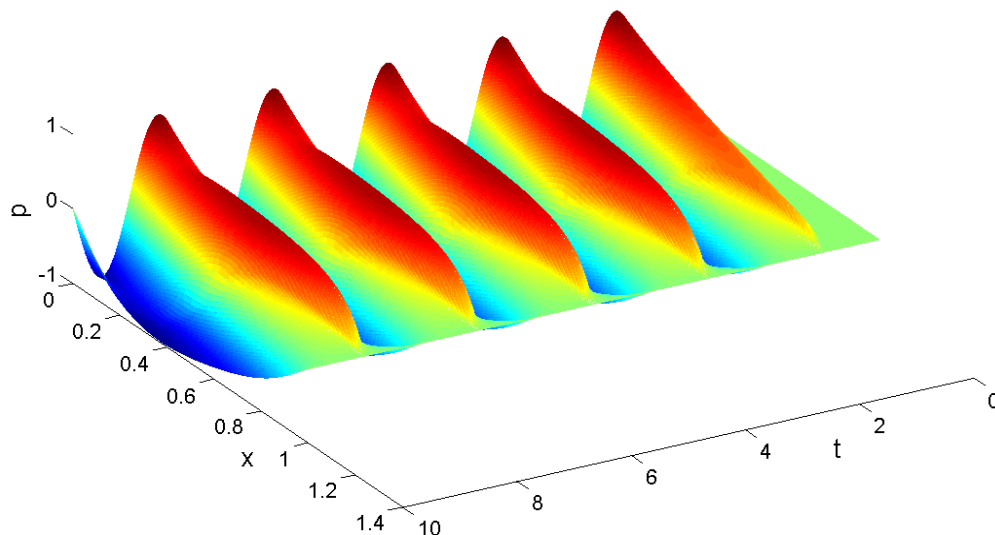
Figure 1 – Acoustic pressure field as a function of space and time for Dirichlet's boundary conditions, α = 5, γ = 1, $n = 1$, ε = 0.2, β = 1, $N = 1001$ and $\Delta t = 0.0001$.

For the same values of the parameters as those of Figure 1 and Neumann's boundary conditions, the results presented in Figure 2 show an initial transient followed by a periodic regime, whereby there is a periodic behavior of the relative maxima and mimima of the pressure at the upstream and downstream boundaries; in fact, when a maximum is observed at the upstream boundary, a minimum can be seen at the downstream one, and vice versa. A similar behavior to that shown in Figure 2 is illustrated in Figure 3 that corresponds to Robin's boundary conditions with $a = b$ in Eq. (5), although the downstream boundary pressure is higher in Figure 3 than in Figure 2.
For the case of no damping and radiation boundary conditions, the results are presented in Figure 4 clearly show compression and expansion waves that propagate along the right-running characteristic and that the initial transient to achieve a periodic behavior is smaller than those of the Neumann's and Robin's boundary conditions which, in turn, require a smaller time to achieve periodicity than the Dirichlet's boundary conditions.
The results presented in Figures 1-4 do not show any numerical instabilities and the pressure field is a smooth function of space and time. For higher nonlinearities, i.e., higher values of $\beta \varepsilon$, it was observed that the time step had to be decreased substantially and small oscillations could

be observed in the pressure field. The amplitude of such oscillations was found to decrease when both the time and spatial step sizes were decreased and, for large values of $\beta \varepsilon$ oscillation-free numerical results could be obtained with 4001 grid points and a time step smaller than 0.00005. As stated above, Eq. (2) changes type at a critical pressure that only depends on $\beta \varepsilon$; for pressures higher than this critical value, Eq. (2) may become locally elliptic and the numerical method presented in this paper cannot cope with such a regime.
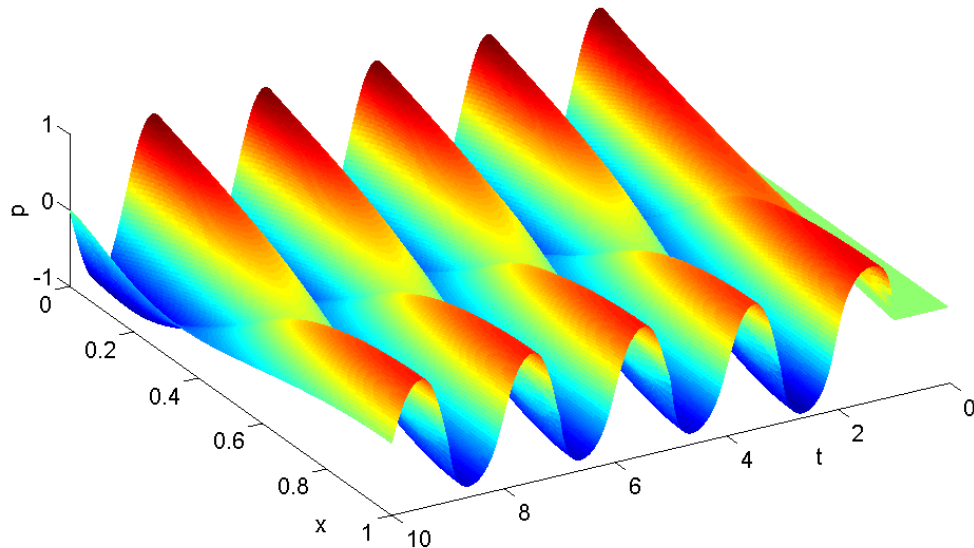
Figure 2 – Acoustic pressure field as a function of space and time for Neumann's boundary conditions, α = 5, γ = 1, $n = 1$, ε = 0.2, β = 1, $N = 1001$ and $\Delta t = 0.0001$.
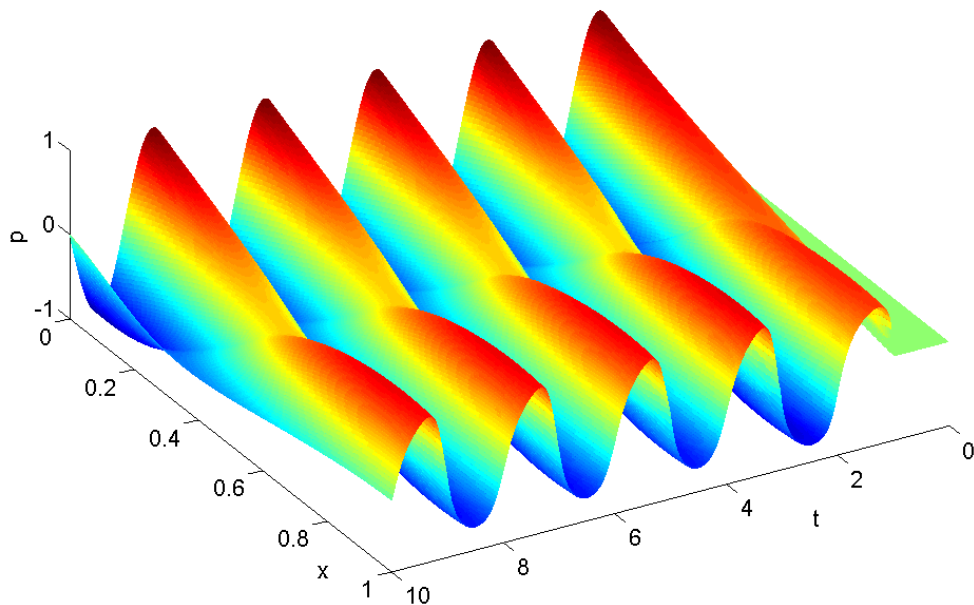
Figure 3 – Acoustic pressure field as a function of space and time for Robin's boundary conditions, α = 5, γ = 1, $n = 1$, ε = 0.2, β = 1, $a = b$, $N = 1001$ and $\Delta t = 0.0001$.
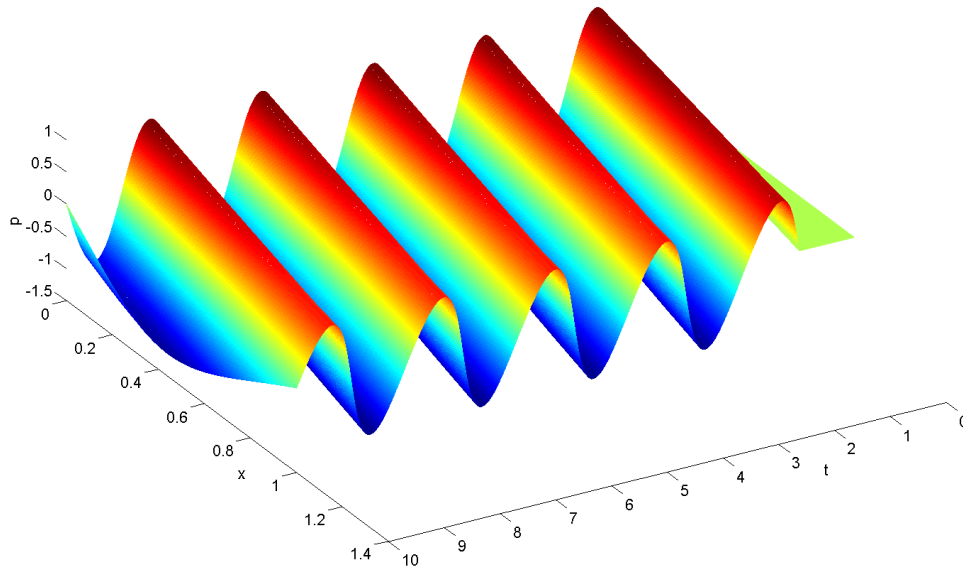
Figure 4 – Acoustic pressure field as a function of space and time for $\mu = 0$ and radiation boundary conditions, α = 0, $n = 1$, ε = 0.2, β = 1, $N = 1001$ and $\Delta t = 0.0001$.

4   Conclusions

A time-domain finite-difference method based on the use of a three-point, fourth-order accurate, compact finite difference discretization of the second-order spatial derivatives, and an explicit, fourth-order accurate Runge-Kutta method for time integration, has been developed to study the effects of the downstream boundary conditions on the acoustic pressure field governed by the nonlinear, one-dimensional, lossless Lighthill-Westervelt equation. It has been shown that, in the presence of a phenomenological damping model, a periodic behavior is observed for both soft- and hard-wall, transmittance and radiation boundary conditions after an initial transient which depends on the damping term and the downstream boundary conditions, when the acoustic pressure at the upstream boundary is sinusoidal. This periodic behavior seems to be analogous to that observed in non-conservative, nonlinear dynamical systems subject to excitation. It was also found that the coefficients of the phenomelogical damping term employed in this study play a paramount role in determining the acoustic pressure field and the interactions of the presure waves with the downstream boundary; in fact, the slope of the pressure at the downstream boundary decreases as the coefficient of the damping term is increased and, in some cases, it is an almost linear function of space at each time.

Acknowledgements

References

[1]   Lighthill, M. J. On sound generated aerodynamically I. General theory. *Proc. Royal Soc. (London), Series A*, Vol. 211, 1952, pp. 564-587.

[2]   Westervelt, P. J. Parametric acoustic array. *J. Acoust. Soc. Am.*, Vol. 35, 1963, pp. 535-537.

[3]   Hamilton, M. F.; Morfey, C. L. Model equations, in: M. F. Hamilton and D. T. Blackstock (eds.), *Nonlinear Acoustics*, pp. 41-63, Academic Press, New York, 1997.

[4]   Beyer, B. T. The parameter B/A, in: M. F. Hamilton and D. T. Blackstock (eds.), *Nonlinear Acoustics*, pp. 25-39, Academic Press, New York, 1997.

[5]   Ramos, J. I.; Nava, E. Numerical solution of the Lighthill-Westervelt equation. Part 1: 1D problems, *Acústica 2012, VIII Congresso Ibero-americano de Acústica*, Évora, Portugal, 1-3 October 2012.

[6]   Demi, L.; van Dongen, K. W. A.; Verweij, M. D. A contrast source method for nonlinear acoustic wave fields with spatially inhomogeneous attenuation, *J. Acoust. Soc. Am.*, Vol. 129 (3), 2011, pp. 1221-1230.

[7]   Huijssen, J.; Verweij, M. D. An iterative method for the compurtation of nonlinear, wide-angle, pulsed acoustic fields of medical diagnostic transducers, *J. Acoust. Soc. Am.*, Vol. 127 (1), 2010, pp. 33-44.

[8]   Kamahura, T.; Ishiwata, T.; Matsuda, K. Model equations for strongly focused finite-amplitude sound beams, *J. Acoust. Soc. Am.*, Vol. 107 (6), 2000, pp. 3035-3046.

[9]   Ying, Y.; Shen, D.; Clement, G. T. Verification of the Westervelt equation for focused transducers, *IEEE Trans. Ultra., Ferro. Freq. Control*, Vol. 58 (5), 2011, pp. 1097-1101.

[10] Aanonsen, S. I.; Barkve, T.;Tjøtta, J. N.; Tjøtta, S. Distortion and harmonic generation in the nearfield of a finite amplitude sound beam, *J. Acoust. Soc. Am.*, Vol. 75 (3), 1984, pp. 749-768.

[11] Purrington, R. D.; Norton, G. V. A numerical comparison of the Westervelt equation with viscous attenuation and a causal propagation operator, *Math. Compu. Simul.*, Vol. 82, 2012, pp. 1287-1297.

[12] Jordan, P. M.; Christov, C. I. A simple finite difference scheme for modeling the finite-time blow-up of acoustic acceleration waves. *Journal of Sound and Vibration*, Vol. 281, 2005, pp. 1207-1216.

[13] Ramos, J. I. Implicit, compact, linearized θ-methods with factorization for multidimensional reaction-diffusion equations. *Applied Mathematics and Computation,* Vol. 94 (1), 1998, pp. 17-43.

[14] Mur, G. Absorbing boundary conditions for the finite-difference approximation of the time-domain electromagnetic field equations, *IEEE Trans. Electromagn. Compat.*, Vol. 23, 1981, pp. 377-382.

[15] Higdon, R. L. Absorbing boundary conditions for difference approximations to the multi-dimensional wave equation, *Mathematics of Computation*, Vol. 47 (176), 1986, pp. 437-459.

[16] Givoli, D.; Neta, B. High-order non-reflecting boundary conditions for dispersive waves, *Wave Motion*, Vol. 37, 2003, pp. 257-271.

[17] Neta, B.; van Joolen, V.; Dea, J. R.; Givoli, D. Application of high-order non-reflecting boundary conditions to linear shallow water models, *Communications in Numerical Methods in Engineering*, Vol. 24 (11), 2008, 1459-1466.

[18] Schneider, J. B.; Ramahi, O. M. The complementary operators method applied to acoustic finite-difference time-domain simulations, *J. Acoust. Soc. Am.*, Vol. 104 (2), 1998, pp. 686-693.